# A critical perspective on 1-D modeling of river processes: Gravel load and aggradation in lower Fraser River

Rob Ferguson[1] and Michael Church[2]

Received 15 January 2009; revised 21 July 2009; accepted 13 August 2009; published 21 November 2009.

[1] We investigate how well a width-averaged morphodynamic model can simulate gravel transport and aggradation along a highly irregular 38-km reach of lower Fraser River and discuss critical issues in this type of modeling. Bed load equations with plausible parameter values predict a gravel input consistent with direct measurements and a sediment budget. Simulations using spatially varying channel width, and forced by dominant discharge or a 20-year hydrograph, match the observed downstream fining well. They reproduce major qualitative features of a 47 year sediment budget and match maximum local rates of aggradation and degradation to well within a factor of 2. Locations and rates of aggradation and degradation are influenced by channel constrictions. Runs for single years of unusually high or low peak discharge suggest that the main transfers of gravel occur in different parts of the reach in different years. One-dimensional morphodynamic modeling of highly nonuniform rivers has serious conceptual limitations but may be a valuable complement to empirical approaches.

**Citation:** Ferguson, R., and M. Church (2009), A critical perspective on 1-D modeling of river processes: Gravel load and aggradation in lower Fraser River, *Water Resour. Res.*, *45*, W11424, doi:10.1029/2009WR007740.

## 1. Introduction

[2] Prolonged aggradation of a river bed over many decades can increase flood risk, harm ecosystems, and threaten crossings and other structures. It occurs when the river's capacity to transport the coarser parts of its load is less than the supply of such sediment from upstream or alongside. One approach to understanding aggradation is to try to model bed material transport along the reach concerned. This is straightforward in principle but complicated in practice and is not yet a routine tool despite the obvious attraction of using models to investigate "what if?" scenarios. The main complications are the need to allow for feedbacks in the system and the fact that the relation of bed load transport rate to flow strength is highly nonlinear so that computations are sensitive to local variability in flow strength and to poorly constrained parameters. Our objective is to illustrate and illuminate these issues by a case study. We discuss how we applied a 1-D (width-averaged) model to the lowermost gravel reach of Fraser River in western Canada and consider how well it reproduces the unusually detailed field data that are available on bed load transport and channel change over several decades in this reach. This does not constitute a formal test of the model since uncertainties exist in the field data as well as the modeling assumptions. Rather, we intend that the comparison will give some new insights into both the behavior of the river and the practical application of this type of model. In particular, we examine the effects of nonuniform channel width and of hydrographs of different size and propose a new way to specify a steady "dominant" discharge that conveys the same gravel flux as a hydrograph.

[3] The rate at which a river transports its bed material depends on what fluid drag is applied to what mixture of grain sizes in the bed surface and is therefore influenced by water discharge, channel gradient, and sediment supply. Modeling bed material transport starts with a flow model, usually 1-D (depth and width averaged) but possibly 2-D (depth averaged), which drives transport rate calculations using equations intended for bed load or total load. The bed on which the flow acts is represented by its elevation and either a single grain size or a distribution of sizes. It may be assumed invariant (fixed-bed model) or allowed to alter over time (morphodynamic model). Morphodynamic models compute local aggradation or degradation from streamwise change in bed load flux and often also use mass conservation of each size fraction to compute coarsening or fining of the bed. This last, most complex, type of 1-D model is used in this paper since we consider that bed composition is adjustable over several decades and acts as an important regulator of bed load transport rate.

[4] Multisize 1-D morphodynamic models of this type can reproduce fairly accurately the transient changes in bed level and composition associated with degradational armoring [*Vogel et al.*, 1992], downstream fining [*Hoey and Ferguson*, 1994; *Cui et al.*, 1996], and meander rectification [*Talbot and Lapointe*, 2002]. They also hold promise for investigating river response to landslide and tributary inputs [*Cui and Parker*, 2005; *Ferguson et al.*, 2006], dam removal [*Cui et al.*, 2006], and base level change [*Verhaar et al.*, 2008]. Their main limitation is that using a width-averaged measure of flow strength in a nonlinear transport equation can lead to underestimation of bed load transport, particularly in braided or meandering gravel bed rivers where flow is

[1]Department of Geography, Durham University, Durham, UK.
[2]Department of Geography, University of British Columbia, Vancouver, British Columbia, Canada.


0043-1397/09/2009WR007740

both close to the threshold of motion and highly nonuniform [*Paola*, 1996; *Ferguson*, 2003]. One response to this problem is to model the flow in one dimension and then distribute sediment transport laterally in some way [e.g., *Yang and Simoes*, 2008; *El kadi Abderrezzak and Paquier*, 2009], but these hybrid approaches cannot generate bar-pool topography or model properly how it steers the flow. Fully 2-D morphodynamic models exist and can be applied at reach scale if a sufficiently detailed digital elevation model is available. In research done in parallel with ours *Li and Millar* [2007] and *Li et al.* [2008] simulated lower Fraser River using a commercial 2-D code (MIKE21C; see Danish Hydraulic Institute, MIKE21C user's guide and scientific documentation, Danish Hydraulic Institute, Horsholm, Denmark, 1999) in fixed-bed mode. As we discuss later, they obtained good fits to some, but not all, measured aspects of the river's behavior. While 2-D river models are conceptually superior to 1-D models and may eventually become standard operational tools, river scientists and managers continue to be interested in 1-D models because they are perceived to require fewer data, and less time and expertise, to set up and run. Here we report an attempt at 1-D morphodynamic modeling of the same reach of Lower Fraser River as *Li et al.* [2008]. This represents a severe test of a width-averaged model which necessarily omits much of the spatial detail included within or predicted by a 2-D model. The questions we set out to answer were how best to set up a 1-D model of a highly nonuniform reach and whether it can reproduce the general pattern and details of annual transport and sedimentation of gravel sufficiently faithfully to be of any scientific or practical value. Rigorous testing of the model is not possible because there are considerable uncertainties in available test data, but we use comparisons with data to evaluate alternative choices about model details.

[5] After outlining the character of the reach, we discuss the main issues involved in constructing a 1-D model of it, including how to specify channel width. We then discuss results obtained with alternative channel geometries and forced by various combinations of steady "dominant" discharge, a 20-year hydrograph, and single-year hydrographs. We conclude with some reflections on how 1-D models perform in this type of application and what insight they give into the behavior of this particular river.

## 2. Lower Fraser River

[6] Fraser River drains 250,000 km$^2$ of western Canada, most of it mountainous. Where it emerges from the mountains at river km 150 (all such distances are measured from the seaward edge of the river's delta), it transports up to 1 Mt a$^{-1}$ (megatons per annum) of gravel depending on the duration and peak discharge of the annual snowmelt hydrograph. Almost all of this gravel is deposited in a 30 km long reach starting at Agassiz (km 130), where hydrometric and sediment measurements were made by the Water Survey of Canada (WSC) from 1966 to 1986. Aggradation in this reach is increasing the risk that flood defenses will be overtopped in extreme events, but removal of gravel to increase channel conveyance could cause major damage to fish habitat [*Church and McLean*, 1994]. Summary characteristics of the river at Agassiz and at the long-term hydrometric station at Mis m 85) are listed in Table 1 on the basis of flow and bed load measurements made by WSC and analyzed by *McLean et al.* [1999]. A gravel budget constructed by *McLean and Church* [1999] from surveyed channel changes between 1952 and 1984 was consistent with the input estimated from direct measurements but implied the reworking within the reach of some 2–3 Mt a$^{-1}$ of bed material, which is far more than the input. This reworking is manifest in substantial variation along the reach in the medium-term aggradation rate, with degradation locally. The possibility that local aggradation may be considerably faster than the overall average has increased the concern about flood risk, so the underlying goal of the 1-D and 2-D transport modeling is to reproduce observed rates and patterns of aggradation and degradation. If this can be achieved, models could be used to evaluate mitigation measures and response to hydrological change.

[7] The channel pattern in the reach is shown in Figure 1. The only significant tributary (Harrison River, km 117) is a lake outlet which adds 5–10% to the discharge of the river but negligible bed load. At km 113–119 the river is divided around a large wooded island (Minto Island) with up to one third of the flow in the southern channel (Minto Channel). Over most of the reach the channel exhibits a "wandering" style [*Desloges and Church*, 1989] with low-order braiding, vegetated islands, and extensive gravel bars superimposed on the riffles (Figure 2). Bars typically grow by lateral accretion of diffuse gravel waves migrating along the channel and often deflect flow toward the opposite side of the river, initiating a new cell of erosion, wave formation, and downstream bar accretion [*Rice et al.*, 2009; *Church and Rice*, 2009]. Bed load does not, then, move through the reach as a continuously mobile carpet but in short steps separated by protracted storage in bars. There is systematic downstream fining along the aggrading profile, and past the confluence of the small Vedder River at the upstream end of Sumas Mountain (km 100) the river becomes a single-thread channel with a predominantly sandy bed. Such a rapid change in grain size over a short distance in the lowermost part of the river must be due mainly to size-selective transport and deposition, not abrasion, since this reach is almost completely uncoupled from adjacent hillslopes, and material arriving from the more confined channel in the mountains has already been exposed to many hundreds of kilometers of transport in higher-energy conditions.

## 3. Critical Choices in Model Specification

[8] Our results were obtained using version 5.0 of the SEDROUT 1-D finite difference code developed and described by *Hoey and Ferguson* [1994], but similar choices are involved in applying any 1-D or 2-D multisize morphodynamic model to a particular river. The time-varying state variables are the bed elevation and grain size distribution (GSD) at each computational cell. The process representation consists of depth-averaged conservation equations for water mass and momentum, a flow resistance equation, and a bed load transport algorithm. Bed level is updated using overall conservation of sediment mass, and bed GSD is updated using separate mass conservation equations for each size class within an active layer. Results depend to some extent on the choice of resistance equation and the value of its free parameter, for example Manning's $n$ or the

**Table 1.** Hydraulic Characteristics of Lower Fraser River at Two Gauging Stations[a]

| | Agassiz | Mission |
|---|---|---|
| Mean discharge ($m^3$ $s^{-1}$) | 2880 | 3410 |
| Mean annual flood (MAF) ($m^3$ $s^{-1}$) | 8800 | 9800 |
| Width at MAF (m) | 510 | 540 |
| Mean depth at MAF (m) | 6.6 | 12.6 |
| Water surface slope | 0.00048 | 0.000055 |
| Bed $D_{50}$, surface/subsurface (mm) | 42/25 | 0.4 |
| Suspended sediment load (Mt $a^{-1}$) | 16.5 | 17.0 |
| Bed load (Mt $a^{-1}$) | 0.28 | 0.15 |
| Gravel load (Mt $a^{-1}$) | 0.23 | 0.0002 |

[a]Data are based on 1966–1986 records of the Water Survey of Canada as reported by *McLean et al.* [1999].

ratio of roughness height to grain size in logarithmic equations. They are also sensitive to the choice of bed load transport equation. Gravel transport equations mostly use shear stress as the driver, calculated from depth and energy slope in 1-D models or a quadratic stress law in 2-D models, and contain a very sensitive free parameter in the form of a threshold or reference Shields stress below which transport is negligible. Multisize models contain at least one other free parameter which controls how threshold stress varies with grain size and require a decision about what minimum grain size to consider.

[9] The initial and boundary conditions in both 1-D and 2-D models comprise the lateral limits of the channel, the initial elevation and GSD of each cell in the model domain, the water and sediment input at the top of the reach and from any tributaries, and the water level at the outflow. Predictions of bed load transport are sensitive to initial state in fixed-bed models but much less so in multisize morphodynamic models where both bed slope (hence flow shear stress) and bed GSD (hence threshold shear stress) can evolve. The downstream boundary condition has only a local effect, but the upstream boundary condition is important since the input of water and sediment is what forces the system. The water inflow can be a hydrograph, a design flood level, or a "dominant" discharge which somehow integrates the effects of the natural hydrological regime. The quantity and size distribution of bed material entering the reach can be specified explicitly if sufficient trustworthy data are available, but a common alternative is to assume that the transport rate of each grain size class is at the capacity rate indicated by the chosen equation.

[10] The remaining boundary condition, whether channel width varies along the reach, and if so how, is very significant in a 1-D model. Discharge increases very little along lower Fraser River, but the high-flow width varies from ~0.5 km at the narrowest sections to ~2 km at the widest. The importance of channel width for 1-D modeling is that, for a given discharge and slope, a wider channel has shallower flow and a lower mean shear stress. If flow resistance is represented by the Manning equation, the bed shear stress $\tau$ is estimated using

$$\tau = \rho g (Qn/w)^{3/5} S^{7/10}, \quad (1)$$

where $\rho$, $g$, $Q$, $n$, $S$, $w$ denote the water density, gravity acceleration, water discharge, Manning coefficient, energy slope, and water surface width, respectively. It follows that a 50% increase in width with $Q$, $S$, $n$ held constant reduces $\tau$ by 22%, and a 50% reduction in width increases $\tau$ by 52%. Width-induced differences in shear stress lead to even bigger differences in predicted bed load transport rate and thus affect morphodynamic evolution. Authors using 1-D models to investigate generic aspects of river behavior have normally used a highly simplified channel geometry in which width is constant [e.g., *Hoey and Ferguson*, 1994] or increases smoothly downstream in line with discharge [*Cui and Parker*, 2005]. We show below that a uniform-width model reproduces the broad features of aggradation in lower Fraser River but does not generate local irregularities in aggradation rate; this will only happen if the model includes spatially variable channel width.

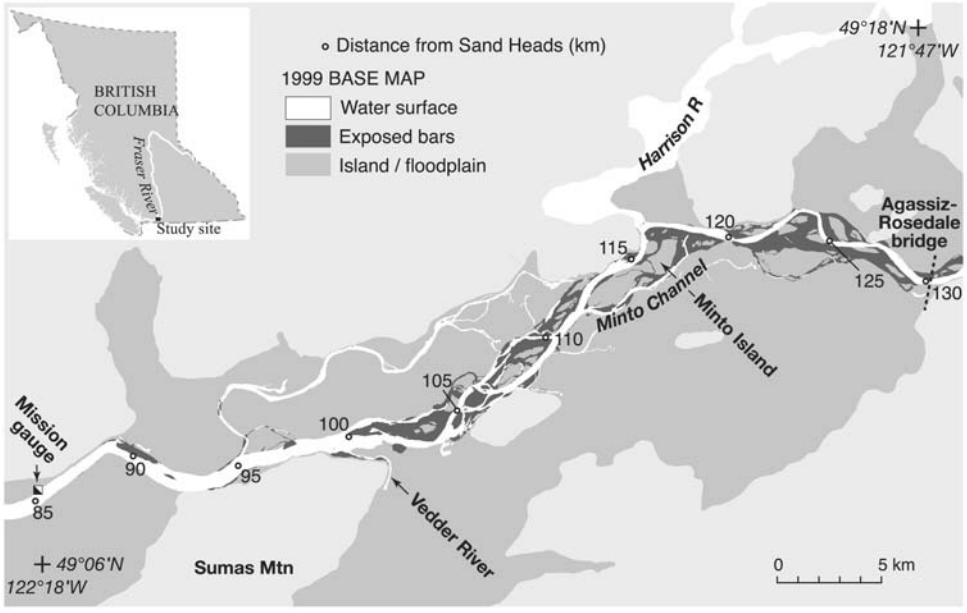


**Figure 1.** Location and key features of the study reach.

**Figure 2.** Oblique view looking down the upper part of the study reach (km 127 to km 117) at moderately high flow showing "wandering" pattern.

[11] Bulk flow properties are best estimated using close approximations of actual cross sections, but, as noted above, this could lead to underestimation of bed load flux to the extent that excess shear stress varies across the channel. *Talbot and Lapointe* [2002] obtained more accurate predictions of bed level change by calculating shear stress from the average of the mean and maximum depths. Another possibility is to reduce the threshold Shields stress and thus increase the excess shear stress and bed load flux. A third stratagem, which we try in this paper, is to use an "effective" width that is lower than the full wetted width and therefore gives higher simulated depth, shear stress, and transport rate per unit width. This approach is conceptually attractive because gravel transport really is restricted to only part of the width in many rivers.

## 4. Constraining the Choices

[12] The critical choices identified in section 3 are interconnected, so another choice is where to begin to narrow the possibilities. Our strategy was to start by specifying grain size range, upstream and downstream boundary conditions, and flow resistance, then choose a bed load transport algorithm to match (perhaps after calibration) empirical evidence about the amount and size composition of the gravel flux into the reach and how they vary with discharge. This makes it possible to estimate a dominant discharge. The definition of effective widths was left until last since doing this in a rational way requires that all the other choices have been made.

### 4.1. Grain Sizes, Upstream Boundary Condition, and Flow Resistance

[13] We used 13 size classes in the model, at 1 phi intervals from 0.5 to 4 mm then half-phi intervals to 128 mm. Grains finer than 0.5 mm are assumed to be washload since they can move in suspension throughout the reach in high flows, though they are in fact common in distal bed samples. Grains up to 2 mm can be suspended at proximal sections in flood conditions but are present in substantial quantities in the bed and move as bed load in weaker flows. As in previous applications of this model [*Hoey and Ferguson*, 1994; *Ferguson et al.*, 2001] we assumed that all deposited bed load is mixed within an active layer of thickness equal to twice its $D_{84}$ grain size. Using a thinner active layer or allowing some deposited sediment to pass through to the subsurface would alter the adaptation rate of the active-layer GSD, but trials show that this has little effect on the eventual state. For reasons explained above no allowance was made for GSD change through abrasion, and with computational nodes that are $\sim$1 km apart we saw no need to allow for any spatial lag in the response of transport rate to flow strength. Bed porosity was set to 0.34 on the basis of field measurements of bulk density which gave a mean of $1.75 \pm 0.11$ t m$^{-3}$.

[14] Although information is available on how bed load flux and its GSD alter with discharge at Agassiz [*McLean et al.*, 1999], there is enormous scatter in the data. Rather than explicitly specifying the sediment input to our model, then, we chose to reserve the sediment rating curve as a test of the model and set the bed load supply to the reach equal to the transport capacity at the first cross section. For simulations forced by hydrographs we used a fixed-elevation boundary condition in which the transport capacity for each size is recalculated at every iteration and the supply is set equal to it, so that there is no change in inlet elevation or bed GSD. However, in simulations forced by steady flow, this assumption led to aggradation at the next few cross sections and therefore a gradual reduction in slope and feed rate at the inlet. To avoid this, we fixed the feed quantity and GSD at their capacity values at the start of the simulation. This still led to gradual aggradation, but at almost the same rate

at the inlet as at the next few sections so that the slope remained almost constant and there was negligible change in bed GSD at the inlet.

[15] The initial bed GSD at the inlet was specified by averaging three 400 pebble surface counts and three 200 kg subsurface bulk samples from locations along a gravel bar whose distal tip is just below the gauging site. The composite GSD has 6% of 0.5–2 mm coarse sand, 8% of 2–8 mm granules, and a main gravel mode centered on 32 mm. The geometric mean diameter ($D_{gm}$) is 22 mm, and the 50th and 84th percentiles ($D_{50}$, $D_{84}$) are 27 and 59 mm. The same GSD was prescribed at all locations along the river initially, leaving the model free to develop a downstream fining profile which can be compared with field measurements.

[16] Flow resistance was assumed to be due only to skin friction, since no dunes or other large bed forms have ever been observed on the extensive parts of the bed that are exposed in winter or in underwater imagery of the talweg. Calculations using the Keulegan equation over the full range of slope and mean depth in the reach, and with roughness height anywhere between 1 and 4 times local bed $D_{84}$, gave results equivalent to a very narrow range of Manning's $n$ (0.026–0.030), so we used the Manning equation with the global value $n = 0.028$ in all simulations. The downstream water level was determined using this value of $n$ and the known water surface slope.

### 4.2. Bed Load Transport

[17] We tried two bed load transport algorithms: those of *Parker* [1990] and *Wilcock and Crowe* [2003], which we refer to hereafter as P90 and WC03. The "straining function" in P90 was modified as described by *Ferguson et al.* [2001] for application to gravel-sand mixtures. The reference Shields stress in the P90 equations, denoted hereafter by $\theta_r$, has a default value of 0.0386 based on field measurements at a single site. The equivalent parameter in WC03 is the reference Shields stress $\theta_{rg0}$ for gravel transport in the absence of sand, with a default value of 0.036 based mainly on flume data. Since the entrainment threshold is known to vary somewhat with bed structure and sand content [e.g., *Church et al.*, 1998; *Wilcock and Crowe*, 2003], we were prepared to vary $\theta_r$ and $\theta_{rg0}$ to some extent to match data on bed load flux and GSD at Agassiz.

[18] The comparison was made by spreadsheet calculations using the bed GSD described above and the daily discharge data for the full 1967–1986 period of record at Agassiz. To do the calculations we also had to specify channel width and slope so that the shear stress could be calculated using equation (1). This would be straightforward except that the water surface slope at Agassiz increases with discharge because of the reduced backwater effect of a riffle ~1 km downstream. Just how much the slope alters is unclear. The 2-D flow model used by *Li et al.* [2008] predicted that it increases from only 0.0002 at 5000 $m^3$ $s^{-1}$ to 0.00125 at 11 000 $m^3$ $s^{-1}$, but field observations suggest a much narrower range: 0.00038 at just under 6000 $m^3$ $s^{-1}$ according to *Sime et al.*'s [2007] analysis of a differential GPS (DGPS) water surface survey and 0.00048 at ~13 000 $m^3$ $s^{-1}$ on the basis of extreme flood levels at stage boards ~1 km apart [*McLean et al.*, 1999]. Our 1-D flow simulations using cross sections surveyed in 1999 were broadly consistent with the field data, with an increase in energy slop 0.00036 at 4000 $m^3$ $s^{-1}$ to 0.00046 once flow goes overbank at 6500 $m^3$ $s^{-1}$ then little further change. Our spreadsheet calculations assumed a linear increase in slope to a maximum of 0.00048 at $Q >$ 8000 $m^3$ $s^{-1}$. We did not want to include floodplains in the cross sections used for the morphodynamic model, since the reduction in width-averaged flow depth and shear stress in overbank conditions gives an unrealistic reduction in transport rate per unit width and has unpredictable consequences for the product of flow width and unit transport rate. We therefore replaced the real inlet cross section by a rectangular one with high sides and a width of 450 m. This is the average of the estimated active width for gravel transport in the real cross section at 6500 $m^3$ $s^{-1}$ (when flow goes overbank and width is 510 m) and 8000 $m^3$ $s^{-1}$ (when slope stops increasing). Active width was estimated by using the P90 hiding function to calculate a critical depth and subtracting this from the simulated water level on the assumption that local shear stress is proportional to flow depth, which is reasonable for this particular section according to the 2-D modeling by *Li and Millar* [2007].

[19] The other problem in calibrating a transport equation to match the measured gravel flux is that the target value is uncertain despite the exceptional amount of information on bed load transport in this river. *McLean et al.* [1999] and *McLean and Church* [1999] obtained almost identical estimates of the long-term average gravel flux at Agassiz by two independent methods: 0.23 Mt $a^{-1}$ (as shown in Table 1) by fitting a bed load rating curve to the WSC measurements then applying it to the 1967–1986 flow duration curve and 0.20 Mt $a^{-1}$ by a sediment budget calculation for 1952–1984. The sediment budget was based on channel change between repeat surveys, corrected for known gravel extraction and for the sand content of bed and banks and assuming negligible gravel transport past Mission on the basis of WSC sampling there. Although these original estimates are in close agreement it is now thought that both are too low. The uncertainty in the sediment budget stems from the imprecision of the fairly coarse digital elevation model (DEM) derived from the 1952 and 1984 survey data, errors in interpolating bank lines between surveyed cross sections, probable underreporting of gravel extraction before monitoring was tightened in the 1990s, and inadequate evidence about bed sand percentage in the lower part of the reach where there are hardly any exposed bars. *Ham* [2005] extended the budget to 1999 using a new and more detailed survey and refined it using improved geographic information system (GIS) techniques (see *Martin and Ham* [2005] for a summary) and additional information on bulk density and sand percentage. The most reliable estimate of average gravel input to the reach is now thought to be 0.39 ± 0.08 Mt $a^{-1}$ for 1952–1999. The long-term hydrometric record at Hope (km 165) shows almost identical mean annual floods for 1952–1984, 1967–1986, and 1952–1999, so it is reasonable to compare these periods. The rating curve estimate is uncertain because the pressure difference sampler used at low to medium flows trapped sand as well as gravel, the basket sampler used at high flows trapped only grains coarser than 6 mm, and full grain-size analyses were performed on only a few samples; *McLean et al.* [1999] therefore had to use the average of these few analyses to correct the majority of measurements. Inspection of the original data also reveals some suspiciously

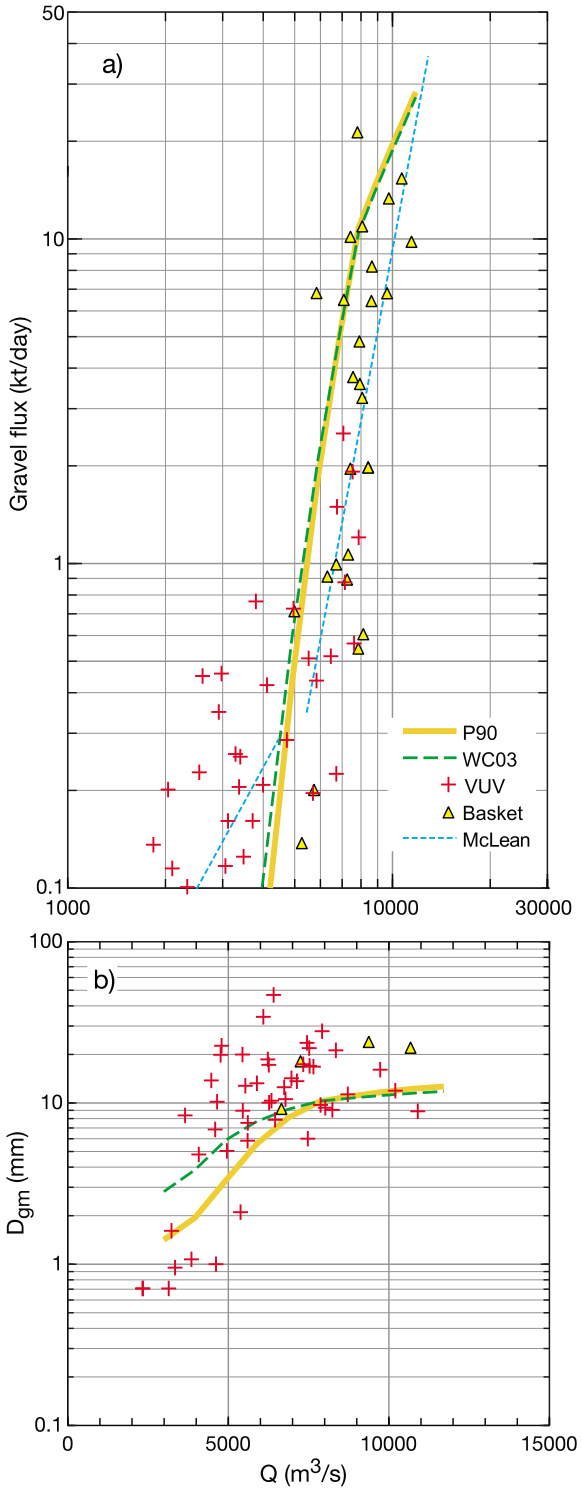


**Figure 3.** Observed and predicted variation of (a) gravel flux and (b) geometric mean bed load grain size with discharge at Agassiz. Data points are measurements by Water Survey of Canada using two types of sampler. Straight lines in Figure 3a are power law ratings fitted by *McLean et al.* [1999] to data at low and high discharge. Curves labeled P90 and WC03 are predictions using the transport equations of *Parker* [1990] and *Wilcock and Crowe* [2003] with reference stress altered as described in the text. The grain size distributions used for Figure 3b were truncated at 0.5 mm.

low or zero fluxes at high discharges; since these are means over five to seven verticals, we think this goes beyond the normal stochasticity of gravel transport and probably shows that the samplers sometimes failed to settle properly on the bottom.

[20] Running the 1967–1986 discharge series through the P90 and WC03 equations with default parameter values and the other assumptions set out above gave mean gravel fluxes of 0.36 Mt $a^{-1}$ and 0.46 Mt $a^{-1}$, respectively. These numbers are already within the uncertainty margin of the 0.39 Mt $a^{-1}$ target and can be brought into exact correspondence with it by very small changes in the reference stresses $\theta_r$ (from 0.0386 to 0.0377) and $\theta_{rg0}$ (from 0.036 to 0.0375). The other test of the transport algorithms is to see how well they reproduce the way gravel flux and its GSD vary with discharge in the WSC data. Figure 3a compares the predicted flux rating curves with the data, and Figure 3b shows how geometric mean bed load diameter varies with discharge. In each case the predictions fall within the scatter of the WSC flux rating at both low and high discharges and within the scatter of the grain-size rating at all but the lowest discharges, so either bed load algorithm is sufficiently versatile for our purposes. We use the P90 equations with $\theta_r = 0.0377$ in the rest of the paper. Repeating some of the runs using WC03 gave very similar results, and the choice does not appear to be critical.

### 4.3. Dominant Discharge and Model Spin-Up

[21] Each member of our main set of simulations had two stages: a spin-up period (called zeroing or priming by some authors [see *Cui et al.*, 2008]), then the run itself. Since our spin-up starts from a state of no downstream fining, with every cross section having the same coarse GSD as the inlet, there is rapid transient adjustment of bed levels and GSDs until downstream fining develops all the way to the outlet of the reach. After this the system is still not in exact equilibrium, but its evolution is much slower. This gradual change in quasi-equilibrium is what is studied in the run itself, with attention focused on the time-averaged local rates of aggradation or degradation (or, equivalently, the time-averaged downstream profile of gravel flux). We used two alternative discharge forcings for the run periods: the actual 1967–1986 hydrograph, or an equivalent period of steady "dominant" discharge as defined below. Runs at dominant discharge were spun up at dominant discharge, but for hydrograph runs we tried both steady and hydrograph spin-up. This gave three combinations of spin-up and run which we refer to below using letter codes dd, dh, and hh, where d denotes dominant discharge, h denotes hydrograph, the first letter denotes the spin-up forcing, and the second letter denotes the run forcing (see Table 2). For consistency, the Harrison River inflow was set to a constant value (700 $m^3$ $s^{-1}$) in all simulations.

[22] We defined dominant discharge as the steady flow which, operating for a suitable fraction of the time, would not only convey the same total quantity of sediment past Agassiz as the 1967–1986 flow series but also give the same overall bed load grain size distribution. To identify this discharge, we calculated daily transport rates of each gravel size class, summed them to obtain the overall size distribution of the estimated 7.8 Mt of gravel conveyed during 1967–1986, then found the geometric mean of this GSD (9.0 mm). A wide range of combinations of magnitude

**Table 2.** Discharge Forcing Scenarios Used in Simulations[a]

| Run Code | Spin-Up Period | Run Period |
|---|---|---|
| dd | dominant discharge | dominant discharge |
| dh | dominant discharge | 1967–1986 hydrograph |
| hh | 1967–1986 hydrograph | 1967–1986 hydrograph |

[a]See text for definition of dominant discharge. Both periods are ~20 years.

and duration of steady discharge could match the 20 year average gravel flux of 0.39 Mt $a^{-1}$, but only one ($Q$ = 7000 $m^3$ $s^{-1}$ for 53 days per year) also gives $D_{gm}$ = 9.0 mm. Simulations using this dominant discharge have a time ratio of 365/53 = 6.88 calendar years per model year. It should be noted that our dominant discharge is conceptually different from the widely used "effective" discharge of *Wolman and Miller* [1960] and will normally have a different value. Our definition is the most appropriate for present purposes since the "effective" discharge does not automatically match the mean or median transport rate [*Vogel et al.*, 2003], nor does it take account of the size distribution of the load. The development of downstream fining throughout the reach took just under 3 model years at a steady 7000 $m^3$ $s^{-1}$, so we adopted 3 model years as the duration of a dominant-discharge spin-up or run. This is equivalent to 20.6 calendar years, so the durations of d- and h-type runs are effectively the same.

[23] Our calculations indicate great interannual variability in gravel input to the reach because of differences in the duration and peak level of the snowmelt hydrograph. The range from minimum (0.03 Mt $a^{-1}$ in 1980) to maximum (1.14 Mt $a^{-1}$ in 1972) is similar to what *McLean et al.* [1999] estimated using rating curves fitted to the WSC bed load measurements. To gain insight into the effects of unusually high or low peak flows we ran 1 year simulations using the 1980 and 1972 hydrographs and two less extreme hydrographs. These runs started from the final state of one of the main runs (dh in Table 2). Flows below 4000 $m^3$ $s^{-1}$, which make up 76% of the 20 year record, are calculated to convey only 0.1% of the total gravel load and were omitted in all simulations using hydrographs.

### 4.4. Channel Width

[24] We ran simulations using three alternative geometries: a "real" geometry based on the surveyed cross sections and having spatially variable width and an irregular long profile, an "effective" geometry consisting of narrower rectangular cross sections with spatially variable width and irregular long profile, and a "uniform" geometry with a simple initial long profile and the same width at all places and times. Simulations using the real and effective geometries were repeated using each of the discharge scenarios listed in Table 2; we prefix the run codes with R or E to distinguish which geometry was used. The uniform geometry was used only with steady discharge (the dd scenario).

[25] The "real" (R) geometry extends for 38 km from Agassiz to a point partway into the sand bed reach. It is based on 45 cross sections at intervals of 0.7–1.2 km that were surveyed in 1999 and are plotted by *Church and Ham* [2004]. For present purposes the sections were simplified slightly and contracted n essary to correct for oblique orientation relative to the talweg flow direction. The inlet section was taken to be rectangular and 450 m wide as explained above. The channels on either side of Minto Island are included as separate talwegs with the same water surface elevation.

[26] The "effective" (E) geometry consists of rectangular sections at the same locations as the real ones but with widths equal to the estimated width of active gravel transport at dominant discharge in the real sections. This calculation was done in the way described above for the inlet (section 4.2), using the water levels, energy slopes, and geometric mean bed grain sizes at the end of a 3-year dominant-discharge spin-up. Once the effective width had been determined, a bed level was computed that preserved the same water surface elevation and wetted cross-section area as in the real-sections simulation so that energy slopes are as similar as possible to those in the real geometry. The active-width calculation implicitly assumes that local shear stress is proportional to local depth. We know from acoustic Doppler current profiler (ADCP) profiles that this is not true in detail but that discrepancies due to deep, gently flowing locations and shallow, fast flowing locations will tend to cancel. The median and maximum effective widths are 800 and 1300 m, compared to median and maximum water surface widths of 965 and 1980 m at the end of the spin-up. We had intended to make the sections trapezoidal with side slopes fixed using a second active-width calculation at a higher discharge, but this procedure sometimes gave an unphysical negative value for the required bottom width and thus was abandoned. With vertical sidewalls the simulated shear stress increases faster with discharge than it does in the real sections.

[27] In the "uniform" (U) geometry the sections are further simplified by standardizing their width at 450 m. This is the approximate active width at the narrowest parts of the river, including Agassiz as discussed above, so using it for the entire length of the reach shows what would happen in the absence of wider sections. A very simple initial bed long profile was specified: a constant high slope of 0.0005 for the first 33 km, then a constant low slope of 0.00005. This gives realistic slopes at Agassiz and Mission and the correct drop between them. The water surface profile at the end of the dominant-discharge spin-up differed little from that in the other two geometries, so any difference in results is due to the different assumptions about channel width.

## 5. Test Data

[28] We illustrate model performance by quantitative comparison with available data, although our evaluations are essentially qualitative because of uncertainties in the data. Simulated gravel fluxes and aggradation rates are compared with those estimated for cells of average length 1 km in the previously mentioned 1952–1999 sediment budget. The empirical aggradation rates were derived from the overall budget by correcting for gravel extraction and the sand content of bed and bank material. They range from $-5$ to $+36 \times 10^3$ $m^3$ $km^{-1}$ $a^{-1}$ and have confidence intervals of $\pm 1$ to $2 \times 10^3$ $m^3$ $km^{-1}$ $a^{-1}$ according to the number of grid points in the cell. Gravel fluxes at cell boundaries were estimated from Mission upward using the mass continuity equation $G_i = G_{i-1} + \Delta S_G$, where $G$ is

gravel flux at section $i$, $S_G$ is gravel accumulation between $i$ and $i-1$, $i$ increases upstream, and $G_0$ is the near-zero $G_0$ at Mission based on the WSC measurements there (Table 1). This calculation gives small negative fluxes at km 102–103, indicating error in either $G_0$ or the budget; we assume the latter. Confidence intervals based on the combined effects of DEM error, uncertainty in sand percentage, and uncertainty in bulk density become wider as the calculation is propagated upstream and reach ±0.08 Mt $a^{-1}$ at Agassiz. When assessing agreement with simulated gravel fluxes, the uncertainty in bulk density cancels, and the confidence interval at Agassiz decreases to ±0.06 Mt $a^{-1}$.

[29] The main test is the way gravel flux is predicted to decline along the reach, since this differs between model runs even though the gravel input has been forced into approximate agreement with the sediment budget through our choices of inlet width and reference stress. We present results both as flux profiles, which allow easy comparison of several runs on one plot, and as aggradation profiles obtained by differencing the flux profiles. Three progressively tougher tests of realism are (1) how well each model reproduces the distance over which gravel transport declines to a negligible level, and thus reproduces the position of the gravel front; (2) whether the combination of width variability and discharge scenario in a run generates a realistic amplitude of local variation in aggradation rate; and (3) how well the loci and rates of maximum aggradation and degradation agree with the field data.

[30] Simulated bed grain size distributions are also of interest since they evolve within the model and can be compared with field data on downstream fining. These data consist mainly of measurements made in 2000–2001 on all major gravel bars exposed during winter low flow. Since the model active layer corresponds to an approximately equal mixture of what is sampled by surface pebble counts and subsurface bulk samples, we use the geometric mean of the surface and subsurface $D_{50}$ values at each site, with the GSDs truncated at 0.5 mm as in the model. The sparse test data below the gravel front are taken from *McLean et al.* [1999]. They comprise one subsurface bulk sample from a small bar and a few bulk samples dredged from the talweg in 1983–1984 and are not truncated since the GSDs are mainly or entirely sand. A recent sampling program confirms that the gravel front is between 1 and 2 km upstream of the Vedder River confluence; below this the bed is sand apart from a few bimodal patches ($D_{50}$ 2–8 mm) and a gravel veneer on small bars near km 98 and 93 (J. Venditti, Simon Fraser University, personal communication, 2009).

## 6. Results

[31] We start by presenting results from the eight main simulations using the survey-based real and effective geometries and the different combinations of steady dominant discharge or 20 year hydrograph for spin-up and run. The results are broadly similar for all combinations of the three controlling factors (geometry, spin-up, and run forcing) but there are many differences in detail, some of which show the systematic influences of the controlling factors. The broad features of the results are best seen by plotting flux profiles from all six runs in one pair of graphs, so we do this first before looking at downstream fining and then aggradation plots. The contra results using the uniform geometry are also illustrated. We then examine the effects of individual hydrographs of high or low peak discharge.

### 6.1. Simulated Flux Profiles

[32] Figure 4 shows how gravel flux is predicted to vary along the reach in the six main runs using the real and effective geometries. Although the curves start at different heights, they have a strong family resemblance, with a generally concave shape on which are superimposed recognizably similar minor irregularities, including small upturns. The irregularities indicate differences in aggradation rate over short distances, and upturns indicate local degradation. The overall concavity implies more rapid aggradation proximally than distally. At least 90% of the gravel input is deposited before the Vedder River confluence in each run, most of it (62–77%) before Harrison River. This is in broad agreement with the sediment budget. The run using the uniform geometry has a very different and much less realistic flux profile: predominantly convex, with no irregularities and the most rapid decline (fastest aggradation) two thirds of the way down the reach.

[33] In each of the real- and effective-geometry runs the flux profile has a shoulder near km 121 before steepening again, which implies two separate loci of rapid proximal aggradation. The flux profile from the sediment budget has a slight upturn here, indicating slight degradation near what is an unusually narrow cross section that experienced bank retreat and toe scour for much of the study period. In the middle part of the reach the simulated profiles decline gently overall but have a local upturn near km 113. This again resembles a feature of the sediment budget profile, probably related to the confluence of Minto Channel with the main river. Each run also predicts an abrupt reduction in gravel flux around km 102, implying a locally high aggradation rate. This may correspond to the similar-sized drop in flux near km 103 in the sediment budget. Beyond km 100 the predicted fluxes are very low and almost constant. Each run plots slightly higher here than the profile from the sediment budget, but the budget profile has a confidence interval of about ±0.01 Mt $a^{-1}$ in this part of the reach and would be higher by >0.02 Mt $a^{-1}$ if recalculated to avoid negative fluxes.

[34] The features mentioned so far are ones which are common to each run and agree fairly well with the sediment budget. There are, however, some systematic discrepancies between simulations and budget, as well as differences between individual runs. The main systematic discrepancy is that all but one of the runs (Rhh) overpredicts the gravel flux in the middle part of the reach, from the Minto Channel confluence toward the Vedder River confluence. We suggest possible explanations for this later. Conversely, the Rhh run drastically underpredicts the flux in the first 10 km of the reach. This is connected with another feature of Figure 4: the substantial differences in the simulated time average input of gravel, which ranges from 18% above the sediment budget estimate in run Rdh to 40% below it in run Rhh. For each combination of spin-up and run forcing, the E geometry input is closer to the budget figure than is the R geometry input. The two lowest inputs, which actually fall outside the confidence interval of the sediment budget estimate, are for the Rhh and Ehh runs that were spun up using the 1967–1986 hydrograph. This is a consequence of the nonuniformity of the proximal part of the channel

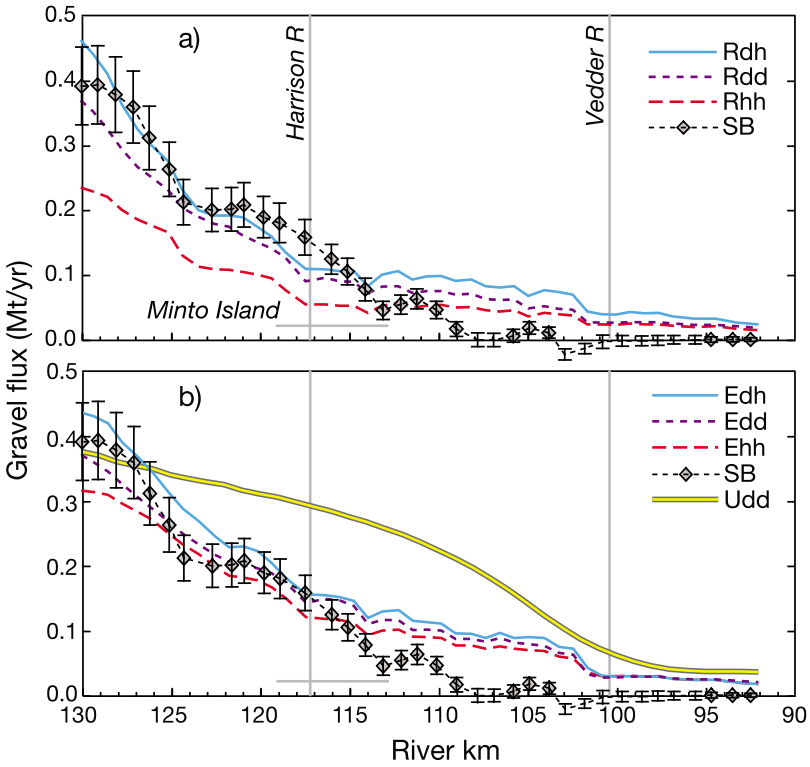


**Figure 4.** Downstream variation in time-averaged gravel flux as predicted in runs using different combinations of dominant discharge and 1967–1986 hydrograph for spin-up and run showing results for the (a) real and (b) effective widths, with the uniform-width run (labeled Udd) added to Figure 4b. The flux profile inferred from the 1952–1999 sediment budget (labeled SB) is shown for comparison, with two standard error uncertainty bars. Vertical lines mark the confluences of Harrison River and Vedder River, and the horizontal bar shows where the river is divided around Minto Island.

combined with the use of a fixed-elevation upstream boundary condition in hydrograph spin-ups and runs. A capacity supply at Agassiz is not a capacity load at the wider sections immediately downstream, so there is differential aggradation and a gradual but progressive decline in slope, transport capacity, and supply to the reach. In runs or spin-ups using dominant discharge, with an invariant feed rate matched to the initial capacity, changes in capacity at Agassiz cause changes in bed level there, and the feedback is smaller and inconsistent: the dd runs have inputs close to the budget value, while the dh runs have inputs higher than the budget.

[35] Although the proximal aggradation rate is high in all six runs, it is systematically highest in runs using the real geometry rather than effective sections. One measure of this is that the proportion of the gravel input that is deposited before Harrison River is 76–77% in R runs, compared to 62–65% in E runs. The difference will be apparent again in section 6.3, where we present and discuss profiles of aggradation rate.

### 6.2. Downstream Fining

[36] Like the gravel flux profiles, downstream fining profiles at the end of each of the six main runs show a strong family resemblance. Figure 5 shows the envelope of these runs with field data for comparison. The simulated pattern agrees rather well with the observations, with an abrupt gravel front in the right place and the correct overall rate of fining above it. Some of the irregularities in the simulation results also match features of the data, including the fining-coarsening-fining alternation at km 125-122-120-117. The main discrepancies are that the model underpredicts $D_{50}$ in midreach (km 116–111) and appears to overpredict it slightly in the last few kilometers of the reach. The midreach discrepancy connects with the previously noted overprediction of gravel flux here, since a finer bed has a lower reference Shields stress and therefore a higher transport rate for the same flow shear stress. The distal discrepancy is more apparent than real: the model excludes sediment finer than 0.5 mm, whereas the dredged field samples here did include it. Although they have medians of 0.3–0.5 mm which cannot be matched by the model, the field samples did contain some gravel.

[37] The uniform-width model predicts a monotonic decline in grain size without the irregularities that are present in the variable-width simulations and field data. The simulated pattern is, however, consistent with the trend of the data as far as km 107. It correctly predicts that the strongest fining is between km 105 and 100, but the grain size at km 105 is slightly underpredicted, and that in the distal reach is considerably overpredicted, so the gravel front is less pronounced than the data suggest. The distal overprediction is a consequence of the unrealistically low width and high simulated shear stress in this part of the reach.

### 6.3. Aggradation Profiles

[38] The gravel flux profiles in Figure 4 are not straight lines, indicating that the predicted local aggradation rate

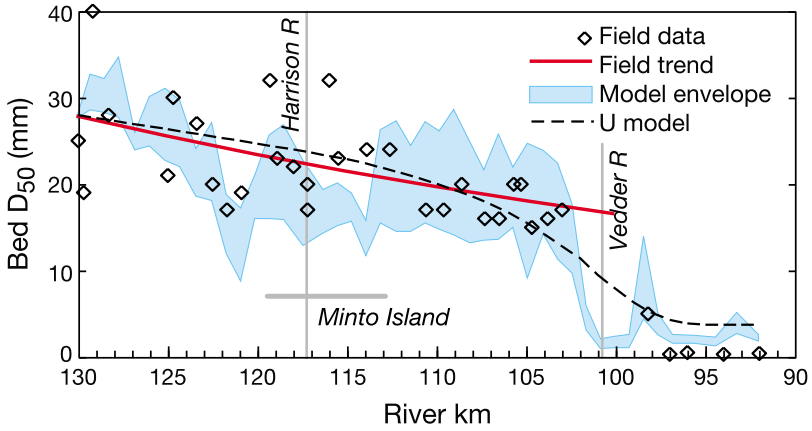


**Figure 5.** Downstream fining along the reach as observed (symbols and best fit exponential trend) and as simulated (envelope of results from six R and E runs and line for the uniform-width run Udd).

varies along the reach. We have already noted some points of qualitative agreement with the sediment budget on the basis of matches between shoulders, reversals, or steepenings in the simulated flux profiles with those in the budget profile. We now make a more detailed comparison in terms of aggradation rates per unit channel length (Figure 6). The empirical rates are taken from the volumetric sediment budget and are plotted at cell-center distances. The simulated rates were obtained by differencing the flux predictions at successive sections, converting from mass to volume, and dividing by the spacing of the sections. They are plotted midway between sections.

[39] The close family resemblance among the six R and E geometry flux profiles in Figure 4 is reflected in a similar resemblance in the corresponding aggradation profiles in Figure 6. As previously discussed, the simulated input to the reach differs between runs, and this leads to differences in overall aggradation rate (since hardly any gravel leaves the reach) as well as big differences in the maximum aggradation rate in the first 10 km of the reach. The extrema in the middle of the reach differ far less between runs. The locations of fastest aggradation are always the same: a prominent proximal peak near km 125, a prominent distal peak at the gravel front near km 102, and lesser peaks near km 118 and km 114. These loci of high simulated aggra-

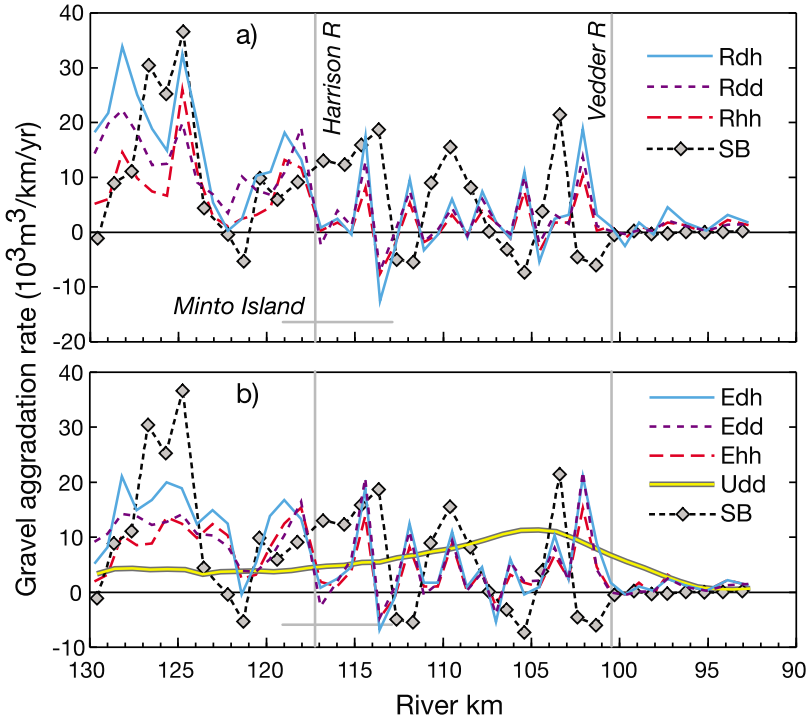


**Figure 6.** Downstream variation in time-averaged gravel aggradation rate as predicted using (a) real geometry and (b) effective geometry, each with different combinations of dominant discharge and 1967–1986 hydrograph for spin-up and run. The uniform-width (Udd) run is added to Figure 6b, and the naturalized gravel aggradation rates from the 1952–1999 sediment budget (SB in legend) are shown for comparison. Con e intervals for the SB rates are no bigger than the symbols.

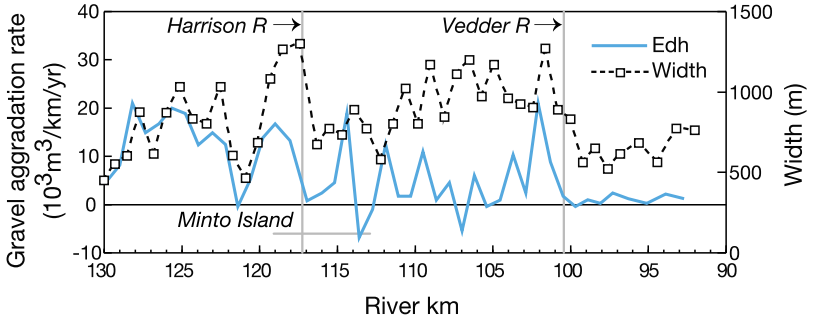


**Figure 7.** Example of the correlation between variable channel width and irregular aggradation rate: run Edh using the 1967–1986 hydrograph in the effective geometry. Aggradation rates are averaged over the hydrograph.

dation rate are separated by loci of minimal change or slight degradation, and there is minimal change below the Vedder River confluence. The uniform-width run shows an entirely different pattern with a low and near-constant rate proximally, a gradual midreach increase to a maximum near km 105, then a progressive decline extending well beyond Vedder River.

[40] The simulated aggradation profiles do not match the sediment budget closely, but several of its key features are reproduced fairly well in the runs using real or effective widths. None of the simulations has such a high maximum aggradation rate as the budget shows near km 125, but the Rdh run gets close, and all runs predict relatively high aggradation thereabouts. Only one run (Edh) predicts slight degradation near km 121, as in the budget, but all six R and E runs correctly predict a local minimum here followed by a rise to a local peak near the Harrison River confluence. The sediment budget, however, shows aggradation continuing to km 114, whereas the simulations show little or no change around km 116–117. The simulations do all reproduce the observed slight degradation near the Minto Channel confluence (~km 113), but they underestimate aggradation over the next few kilometers. The major aggradation peak at the gravel front is matched well in amplitude, but the model puts it slightly further downstream than in the budget. Beyond km 100 the model with R or E geometry correctly predicts very little gain or loss of gravel, whereas the uniform-width run incorrectly predicts significant aggradation. Because aggradation rates are estimated at different sets of locations in the model and in the budget, there is no simple quantitative method for deciding which simulation gives the best agreement with the budget, but the uniform-width run is clearly the worst by far. The greatest differences between the real- and effective-width runs are in the first 10 km of the reach, and here the hydrograph runs preceded by steady spin-up (Rdh and Edh) give the closest visual match to the budget. The Rdh run comes closest to matching the budget estimate of the range of local aggradation rates ($-13$ to $+34 \times 10^3$ m$^3$ km$^{-1}$ a$^{-1}$ simulated, $-7$ to +36 observed).

[41] The simulations would not produce irregular aggradation profiles without the spatial variability in width that exists in the R and E geometries, but, as Figure 7 shows, the link between width and aggradation is not just a matter of aggradation at wide sections and degradation at narrow sections. Aggradation can be quite slow where the channel is uniformly wide, as between km 110 and 105. It is streamwise change in width that matters: the highest aggradation rates occur in channel expansions, typically just before the widest section (e.g., km 119 and 102), and degradation occurs in channel constrictions, typically just upstream of the narrowest section (e.g., km 121 and 117).

### 6.4. Effects of Single Hydrographs

[42] The final set of simulations looked at the effects of a single annual hydrograph with an unusually high or low peak discharge. The starting point for each run was the final state of the Rdh or Edh simulation since, as just noted, these gave the most realistic 1967–1986 aggradation profiles. The chosen hydrographs were those for 1972 (highest peak discharge and gravel flux), 1974 (above-average peak discharge, flux about double the average), 1973 (below-average peak, flux about half average), and 1980 (lowest peak discharge and gravel flux). Discharge below km 117 was supplemented by 700 m$^3$ s$^{-1}$ to allow for the Harrison River inflow. The flux profiles obtained by integration over each hydrograph are shown in Figure 8. As would be expected from the differences in peak discharge, the calculated capacity input of gravel to the reach varies enormously: only one tenth of the dominant-discharge input in 1980 but over three times higher in 1972. This range is roughly the same as in our spreadsheet calculations (section 4.3) and *McLean et al.*'s [1999] rating curve calculations, though the modeled fluxes are generally higher than those from the rating curve.

[43] The most significant feature of Figure 8 is that, while each hydrograph generates local degradation in several places, the locations differ between hydrographs. For example, km 120–122 experiences degradation in high-peak years (and in the long-term sediment budget) but aggradation in low-peak years, whereas km 118–119 shows the opposite pattern. This may explain why the 1967–1986 sequence of different hydrographs redistributes gravel within the reach in a smoother way than any of these four individual hydrographs. The single-hydrograph runs predict that most of the large gravel supply in years of high peak flow is deposited within the first 13 km to Harrison River, but in years of below-average peak flow there is little aggradation in this proximal subreach, or even net degradation as relatively fine material is winnowed from the bed. Beyond Harrison River the flux profiles gradually converge to almost identical low values at the gravel front around km 101, but below this they diverge again: what gravel is present in the head of the sand bed reach is mobilized in

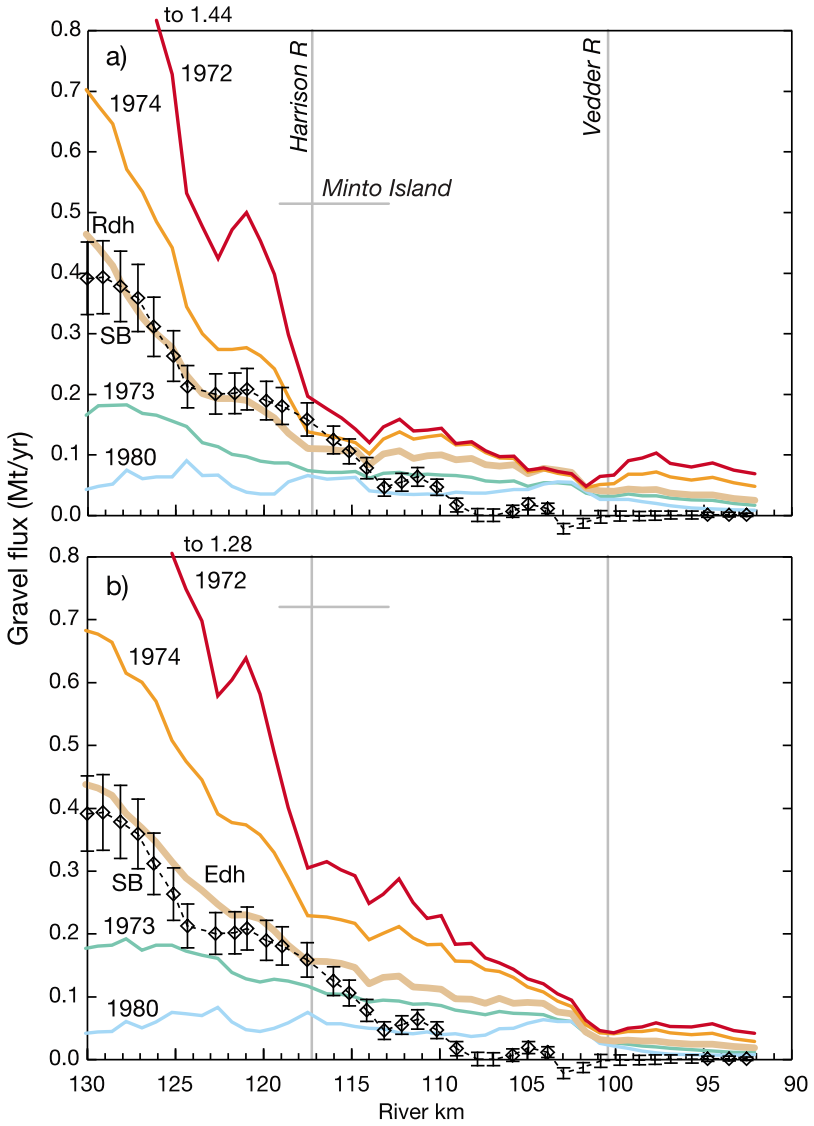


**Figure 8.** Simulated gravel flux profiles averaged over single-hydrograph runs in (a) the real geometry and (b) the effective geometry. Each run started from the final state of the Rdh or Edh simulation and is labeled with the year of the hydrograph. The mean 1952–1999 flux as inferred from the sediment budget (SB) and the mean 1967–1986 flux predicted in the Rdh or Edh run are shown for comparison.

high peaks, with much of it exported from the model reach, whereas in low-peak years most of the gravel that enters the sand bed reach is deposited within the first 5–10 km. Dividing the total gravel flux into rising and falling limb components (not illustrated) reveals that they are often out of phase, implying a seasonally reversing pattern of scour and fill. For the most part it takes the form of rising limb scour in the approach to a constriction, accompanied by deposition in the ensuing expansion, followed by deposition in the contraction as discharge falls again and in places also some scour of the expansion. These changes are accompanied by perceptible coarsening and fining of bed material, and the changes on the falling limb do not always cancel those on the rising limb.

## 7. Discussion

[44] One-dimensional modeling of a river as nonuniform as the lower Fraser has obvious conceptual limitations. A width-averaged model cannot simulate the details of flow, bed load transport, or channel change in bar-pool-riffle units, and because it does not allow for cross-stream variation in flow strength, it will tend to underestimate the width-integrated bed load transport capacity. The assumption in our model that each cross section retains the same width throughout the simulation period is also unrealistic. Yet our results suggest that a 1-D morphodynamic model can capture important aspects of reach-scale behavior over tens of years. The simulated patterns of downstream decline in gravel flux and corresponding patterns of aggradation/degradation (Figures 4 and 6) are broadly realistic, and the model predicts a sharp gravel front exactly where it occurs in the field (Figure 5).

[45] One factor contributing to the realism of the simulations is that the transport capacity equations of *Parker* [1990] and *Wilcock and Crowe* [2003] appear to work well in this river. Transport equations can be made to predict any desired average load by calibrating their parameters (or, in a

1-D model, the width used for the calculations), but in this case the P90 and WC03 equations match the empirical estimates of average gravel input with minimal calibration and also match quite well the observed rating curves of load and caliber (Figure 3). Realism over a wide range of discharge and shear stress at the head of the reach makes it possible to simulate the effects of hydrographs and increases confidence that the equations will also work well further downstream.

[46] Another factor is our use of a full morphodynamic model rather than a sediment transport model in which bed grain size distributions (GSDs) are fixed on the basis of available data. Morphodynamic modeling allows for a feedback which we think is important over extended time and space scales: the possibility of local coarsening or fining of the river bed through size-selective entrainment or deposition. Aggradation is typically accompanied by surface fining, degradation by surface coarsening. The consequent changes in the threshold flow for significant transport tend to reduce streamwise differences in transport capacity. All this is modeled with full mass conservation of each size of bed material. We would have little confidence in a morphodynamic model which predicted sediment flux and aggradation well only by virtue of highly unrealistic adjustments to grain size, but in this application the models with real or effective channel widths get both the aggradation profile and the downstream-fining profile approximately right. It is interesting to note that the conceptually superior 2-D model used by *Li and Millar* [2007] and *Li et al.* [2008], again with the P90 transport equations but using fixed bed size distributions, did not reproduce the observed aggradation profile very well. There was good agreement with the flux rating curve, and realistic spatial patterns of bed shear stress and bed load transport intensity at Agassiz, but the simulated gravel flux profiles at each of a range of steady high flows [*Li et al.*, 2008, Figure 7] contain far bigger fluctuations than in our simulations or the 1952–1999 sediment budget. Moreover, the peaks and troughs are in the same places at each discharge, which implies unrealistically high local rates of aggradation and degradation when integrated over a year or more. This could be because the bed composition in the unsampled deeper parts of the channel is not the same as on the bars or alters during hydrographs. Running the 2-D model in full morphodynamic mode to generate its own bed would allow for these possibilities, though both *Li et al.* [2008] and *Ferguson* [2008] found that this particular model gives unrealistic shear stress predictions around bar margins.

[47] Despite a great deal of careful work over a long period the empirical data are insufficiently precise for any rigorous model testing. The gravel aggradation rates given by the sediment budget are subject to uncertainty not just because of the inevitable DEM error but also because sand percentages measured at a few bar-top sites have to be extrapolated to the entire channel area, including talwegs. The sediment budget estimate of the mean annual gravel supply to the reach in 1952–1999 has an uncertainty exceeding ±20%, and it differs considerably from previous estimates of the 1952–1984 average [*McLean et al.*, 1999] even though the post-1984 period was hydrologically similar. A definitive test of this or any other model would require not just repeat surveys but also more detailed and spatially extensive grain size information and intensive direct measurements of bed load input over the period. These uncertainties in the data used either to set up or to test the model make it hard to be sure that discrepancies between predictions and observations reflect limitations of the model. This is likely to be a problem in any attempt at reach-scale river modeling; see *Ferguson* [2008] for a more general discussion.

[48] Three systematic discrepancies between model predictions and empirical evidence probably do reflect limitations of the model. First, the distal bed, which in fact is predominantly sandy, is simulated as containing 30–60% gravel and thus has a slightly higher gravel flux than the sediment budget suggests. This is a consequence of omitting sediment finer than 0.5 mm from the model. Second, the tendency to underestimate bed $D_{50}$ between Harrison River and the confluence of Minto Channel, and hence to overestimate gravel flux here, could be due to treating what are actually independent channels either side of Minto Island as a single wide channel. In reality Minto Channel conveys no more than one third of the flow and very little gravel, and the $D_{50}$ test data are entirely from the main northern channel. Steady-flow simulations in which Minto Channel is treated as a branch channel conveying water but not bed load give better predictions of downstream fining in the main channel, but their predictions about flux are untestable because the sediment budget is for the entire width of the river, not just the main channel. Finally, although the variable-width models predict maximum and minimum rates of aggradation that can be recognized as approximating to maxima and minima in the sediment budget, the locations are usually out by around 1 km. This may be the best that can be expected when a model based on a snapshot channel configuration is compared with the budget for a 47 year period during which the channel configuration changed considerably, but it is probably also because width-averaged calculations force aggradation and degradation into a longitudinal sequence, whereas what is often observed is erosion on one side of the channel and deposition opposite [e.g., *Church and Rice*, 2009, Figure 5].

[49] The other main discrepancy is that for several kilometers above the gravel front the model predicts higher gravel fluxes than the sediment budget suggests. This may stem from our assumption that the river bed has the same porosity everywhere. In this part of the reach the bed is bimodal, with 25–30% sand within a gravel framework. The pore-filling model of *Frings et al.* [2008] suggests that porosity is typically only ~0.2 in this kind of river bed, which would make the bulk density 20% higher than we assumed. The surveyed volumetric aggradation would then correspond to a significantly greater mass of gravel and give a steeper increase in flux up this part of the reach, bringing the sediment-budget flux profile into closer agreement with the model flux profiles.

[50] We expected the real cross sections to give more realistic results than the idealized uniform-width geometry and "effective" sections to work best of all. The uniform-width run reproduces the length of the aggrading gravel wedge fairly well but not the observed downstream alternation of rapid aggradation with slow aggradation or slight degradation. This confirms the need to take account of spatial variation in channel width, which modulates the

underlying pattern of downstream decline in flow strength as the river approaches base level and causes local adjustments of bed level (i.e., aggradation or degradation) and surface grain size distribution. For example, the increase in width below the head of the reach causes more rapid proximal aggradation and downstream fining than is generated in the uniform-width model. We expected the real geometry to exaggerate the rate of aggradation here, since using the full width of the river in a 1-D calculation tends to underestimate transport capacity, but in fact the predictions agree well with the sediment budget for this part of the reach, whereas the effective geometry underestimates the proximal aggradation rate. Possible reasons for this are that in steady-discharge runs the real-sections model slightly exaggerates downstream fining over the first 10 km, thus reducing threshold shear stresses to compensate for unrealistically high active widths, and that in hydrograph runs the vertical sidewalls of the effective sections lead to exaggerated shear stress and transport capacity at high discharges.

[51] Runs forced by the 1967–1986 hydrograph give quite similar results to runs in the same geometry but forced by steady dominant discharge. This suggests that our definition of dominant discharge (section 4.3) has merit and might be useful in other quantitative studies of gravel transport. The differences that do exist between hydrograph runs and steady runs are partly due to our inability to ensure exactly the same gravel supply in each run, for reasons discussed in sections 4.1 and 5.1 and accentuated by the increase in width below the inlet. In spin-ups and runs using hydrographs there is the further complication that proximal slope varies with discharge. One lesson for future work is that setting up a 1-D model is much easier if the inlet is in a uniform reach, which was not possible in this study. Spinning the model up at steady dominant discharge gave better results in this application, but these issues would repay further investigation.

[52] The runs using single-year hydrographs show interesting differences from those using the 1967–1986 hydrograph. The 20 year runs generate aggradation profiles with approximately the same amplitude of spatial variation as in the 47 year sediment budget (Figure 6). The single-year simulations (Figure 8) suggest that the long-term-average behavior masks much stronger scour and fill in some years and differences between years in the locations of maximum aggradation and of degradation. The steepest parts of the 1974 and 1972 flux profiles correspond to aggradation at twice (1974) or three times (1972) the maximum rate in the long-term budget, and in both the 1972 (highest peak discharge) and 1980 (lowest peak discharge) simulations degradation occurs at several more cross sections than in either the 20 year simulation or the sediment budget. This suggests that most of the gravel entering the reach does so in years of unusually high and/or prolonged peak flow, and it is then redistributed in years of average or below-average peak flow. Since the within-reach patterns of aggradation and degradation differ from year to year, the longer-term flux profile is smoother. These results also imply that a change in hydrological regime could affect not only the overall rate of aggradation but also the locations of maximum change.

[53] We return finally to the absence of any major inconsistencies between the predictions of the variable-width models and the fieldwork-based estimates of flux, aggradation, and grain size. This does not prove that either approach is accurate and reliable, but it does increase confidence that the observed sediment budget is not significantly biased and that the computations truly capture significant elements of the morphodynamics of the river.

## 8. Conclusions

[54] We have applied the 1-D morphodynamic model SEDROUT to a 38 km gravel bed reach of lower Fraser River and compared its predictions with the exceptionally detailed available information on bed granulometry and multidecade channel change and bed load flux. The reach exhibits a complex wandering style, so this is a challenging application for a 1-D model. Although the data set still has limitations that preclude formal quantitative testing of the model, we have established the following main conclusions.

[55] 1. Careful selection of model parameters and boundary conditions is critical. In particular, the upstream boundary condition must reflect in as many respects as possible the observed conditions in the river. This is not easy when, as here, the reach immediately downstream from the inlet is not uniform.

[56] 2. A simple uniform-width model, as often adopted in 1-D calculations, generates a qualitatively correct sedimentary response to approaching base level but fails to reproduce geomorphologically and practically important details of the spatial pattern of aggradation.

[57] 3. Simulations using surveyed cross sections, and forced by steady flow or a 20 year hydrograph, reproduce the observed peak rates of aggradation and degradation to within $\sim$1 km in location and well within a factor of 2 in amplitude. Simulations using variable-width rectangular "effective" sections reproduce local degradation well but underestimate peak rates of aggradation.

[58] 4. Simulations using annual hydrographs of different peak discharge generate different spatial patterns of scour and fill, with major floods supplying most of the long-term gravel load and minor floods redistributing it.

[59] 5. Despite this complex behavior in unsteady-flow simulations, runs at a steady dominant discharge (defined here as matching both the mean gravel input over a 20 year period and its grain size distribution) generate broadly similar aggradation patterns to runs using the 20 year hydrograph. Our definition of dominant discharge may be of value in empirical analyses of gravel transport as well as for modeling.

[60] 6. Model behavior averaged over a 20 year run, whether with steady or unsteady flow, is not wholly independent of how the model is spun up. Spin-up using steady dominant flow gave the most consistent results.

[61] 7. The grain size distribution of the river bed is a key regulator of transport rates, and we think that allowing it to change over time adds to the realism of reach-scale medium-term models. Fractional sediment flux calculations are mandatory for this.

[62] 8. Further progress in understanding model capacity to simulate the behavior of complex river channels requires as much attention to improving field observations and representing them appropriately in the model as to refining the models themselves. Numerical modeling is not a substitute for empirical approaches to understanding and quan-

tifying gravel transport, but it can be a useful complement to them, generating qualitative hypotheses about what may be going on and pointing to important uncertainties in empirical knowledge as well as allowing what if calculations.

[63] **Acknowledgments.** This paper makes extensive use of data carefully gathered over many years by hydrometric personnel of the Water Survey of Canada, supervised for much of the period by Bruno Tassone, by survey personnel of the Canada Department of Public Works and Government Services supervised by Gouin Barford, and by students at the University of British Columbia. Among the latter David McLean, Darren Ham, and Hamish Weatherly deserve special mention for major contributions. UBC work was supported by the Natural Sciences and Engineering Research Council of Canada, which also supported the first author's involvement in the modeling work, and by the Canada Department of the Environment Inland Waters Branch and grants to the City of Chilliwack from the British Columbia Emergency Flood Fund. We also thank Yantao Cui, Jim Pizzuto, and Alain Recking for constructive and thought-provoking reviews which helped us improve the paper.

## References

Church, M., and D. Ham (2004), Atlas of the alluvial gravel-bed reach of Fraser River in the lower mainland, report, 55 pp., Dep. of Geogr., Univ. of B. C., Vancouver, B. C., Canada. (Available at http://www.geog.ubc.ca/fraserriver)

Church, M., and D. G. McLean (1994), Sedimentation in lower Fraser River, British Columbia: Implications for management, in *The Variability of Large Alluvial Rivers*, pp. 221–241, Am. Soc. Civ. Eng., New York.

Church, M., and S. P. Rice (2009), Form and growth of bars in a wandering gravel-bed river, *Earth Surf. Processes Landforms*, *34*, 1422–1432, doi:10.1002/esp.1831.

Church, M., M. A. Hassan, and J. F. Wolcott (1998), Stabilizing self-organized structures in gravel-bed stream channels: Field and experimental observations, *Water Resour. Res.*, *34*, 3169–3179, doi:10.1029/98WR00484.

Cui, Y., and G. Parker (2005), Numerical model of sediment pulses and sediment-supply disturbances in mountain rivers, *J. Hydraul. Eng.*, *131*, 646–656, doi:10.1061/(ASCE)0733-9429(2005)131:8(646).

Cui, Y., G. Parker, and C. Paola (1996), Numerical simulation of aggradation and downstream fining, *J. Hydraul. Res.*, *34*, 185–204.

Cui, Y., G. Parker, C. Braudrick, W. E. Dietrich, and B. Cluer (2006), Dam removal express assessment models (DREAM). Part 1: Model development and validation, *J. Hydraul. Res.*, *44*(3), 291–307.

Cui, Y., J. K. Wooster, J. G. Venditti, S. R. Dusterhoff, W. E. Dietrich, and L. S. Sklar (2008), Simulating sediment transport in a flume with forced pool-riffle morphology: Examinations of two one-dimensional numerical models, *J. Hydraul. Eng.*, *134*(7), 892–904, doi:10.1061/(ASCE)0733-9429(2008)134:7(892).

Desloges, J. R., and M. Church (1989), Canadian landform examples: Wandering gravel-bed rivers, *Can. Geogr.*, *33*, 360–364, doi:10.1111/j.1541-0064.1989.tb00922.x.

El kadi Abderrezzak, K., and A. Paquier (2009), One-dimensional numerical modeling of sediment transport and bed deformation in open channels, *Water Resour. Res.*, *45*, W05404, doi:10.1029/2008WR007134.

Ferguson, R. I. (2003), The missing dimension: Effects of lateral variation on 1-D calculations of fluvial bedload transport, *Geomorphology*, *56*, 1–14, doi:10.1016/S0169-555X(03)00042-4.

Ferguson, R. (2008), Gravel-bed rivers at the reach scale, in *Gravel-Bed Rivers VI: From Process Understanding to River Restoration*, edited by H. Habersack, H. Piegay, and M. Rinaldi, pp. 33–53, Elsevier, Amsterdam.

Ferguson, R. I., M. Church, and H. Weatherly (2001), Fluvial aggradation in Vedder River, British Columbia: Testing a one-dimensional sedimentation model, *Water Resour. Res.*, *37*, 3331–3347, doi:10.1029/2001WR000225.

Ferguson, R. I., J. R. Cudden, T. B. Hoey, and S. P. Rice (2006), River system discontinuities due to lateral inputs: Generic styles and controls, *Earth Surf. Processes Landforms*, *31*(9), 1149–1166, doi:10.1002/esp.1309.

Frings, R. M., M. G. Kleinhans, and S. Vollmer (2008), Discriminating between pore-filling load and bed-structure load: A new porosity-based method, exemplified for the River Rhine, *Sedimentology*, *55*(6), 1571–1593, doi:10.1111/j.1365-3091.2008.00958.x.

Ham, D. G. (2005), Morphodynamics and sediment transport in a wandering gravel-bed channel: Fraser River, British Columbia, Ph.D. thesis, 272 pp., Univ. of B. C., Vancouver, B. C., Canada. (Available at http://www.geog.ubc.ca/fraserriver)

Hoey, T. B., and R. Ferguson (1994), Numerical simulation of downstream fining by selective transport in gravel-bed rivers: Model development and illustration, *Water Resour. Res.*, *30*, 2251–2260, doi:10.1029/94WR00556.

Li, S. S., and R. G. Millar (2007), Simulating bed-load transport in a complex gravel-bed river, *J. Hydraul. Eng.*, *133*(3), 323–328, doi:10.1061/(ASCE)0733-9429(2007)133:3(323).

Li, S. S., R. G. Millar, and S. Islam (2008), Modelling gravel transport and morphology for the Fraser River gravel reach, British Columbia, *Geomorphology*, *95*, 206–222, doi:10.1016/j.geomorph.2007.06.010.

Martin, Y., and D. Ham (2005), Testing bedload transport formulae using morphologic transport estimates and field data: Lower Fraser river, British Columbia, *Earth Surf. Processes Landforms*, *30*, 1265–1282, doi:10.1002/esp.1200.

McLean, D. G., and M. Church (1999), Sediment transport along lower Fraser River: 2. Estimates based on the long-term gravel budget, *Water Resour. Res.*, *35*(8), 2549–2559, doi:10.1029/1999WR900102.

McLean, D. G., M. Church, and B. Tassone (1999), Sediment transport along lower Fraser River: 1. Measurements and hydraulic computations, *Water Resour. Res.*, *35*, 2533–2548, doi:10.1029/1999WR900101.

Paola, C. (1996), Incoherent structure: Turbulence as a metaphor for stream braiding, in *Coherent Flow Structures in Open Channels*, edited by P. J. Ashworth, S. J. Bennett, J. L. Best, and S. J. McLelland, pp. 705–723, John Wiley, Chichester, U. K.

Parker, G. (1990), Surface-based bedload transport relation for gravel rivers, *J. Hydraul. Res.*, *28*, 417–436.

Rice, S. P., M. Church, C. L. Wooldridge, and E. J. Hickin (2009), Morphology and bars in a wandering gravel-bed river; lower Fraser river, British Columbia, Canada, *Sedimentology*, *56*(3), 709–736, doi:10.1111/j.1365-3091.2008.00994.x.

Sime, L. C., R. I. Ferguson, and M. Church (2007), Estimating shear stress from moving-boat acoustic Doppler velocity measurements in a large gravel-bed river, *Water Resour. Res.*, *43*(3), W03418, doi:10.1029/2006WR005069.

Talbot, T., and M. Lapointe (2002), Numerical modeling of gravel bed river response to meander straightening: The coupling between the evolution of bed pavement and long profile, *Water Resour. Res.*, *38*(6), 1074, doi:10.1029/2001WR000330.

Verhaar, P. M., P. M. Biron, R. I. Ferguson, and T. B. Hoey (2008), A modified morphodynamic model for investigating the response of rivers to short-term climate change, *Geomorphology*, *101*, 674–682, doi:10.1016/j.geomorph.2008.03.010.

Vogel, K. R., A. van Niekerk, R. L. Slingerland, and J. S. Bridge (1992), Routing of heterogeneous sediments over movable bed: Model verification, *J. Hydraul. Eng.*, *118*(2), 263–279, doi:10.1061/(ASCE)0733-9429(1992)118:2(263).

Vogel, R. M., J. R. Stedinger, and R. P. Hooper (2003), Discharge indices for water quality loads, *Water Resour. Res.*, *39*(10), 1273, doi:10.1029/2002WR001872.

Wilcock, P. R., and J. C. Crowe (2003), Surface-based transport model for mixed-size sediment, *J. Hydraul. Eng.*, *129*(2), 120–128, doi:10.1061/(ASCE)0733-9429(2003)129:2(120).

Wolman, M. G., and J. P. Miller (1960), Magnitude and frequency of forces in geomorphic processes, *J. Geol.*, *68*(1), 54–74, doi:10.1086/626637.

Yang, C. T., and F. J. M. Simoes (2008), GSTARS computer models and their applications, part I: Theoretical development, *Int. J. Sediment Res.*, *23*(3), 197–211, doi:10.1016/S1001-6279(08)60019-0.

M. Church, Department of Geography, University of British Columbia, 217-1984 West Mall, Vancouver, BC V6T 1Z12, Canada. (mchurch@geog.ubc.ca)

R. Ferguson, Department of Geography, Durham University, South Road, Durham DH1 3LE, UK. (r.i.ferguson@durham.ac.uk)